Kinetic Mechanism of Histidine-Tagged Homocitrate Synthase from *Saccharomyces cerevisiae*†

Babak Andi, Ann H. West, and Paul F. Cook*

Department of Chemistry and Biochemistry, University of Oklahoma, 620 Parrington Oval, Norman, Oklahoma 73019

Received June 14, 2004; Revised Manuscript Received July 16, 2004

ABSTRACT: Kinetic data have been collected suggesting a preferred sequential ordered kinetic mechanism for the histidine-tagged homocitrate synthase (HCS) from *Saccharomyces cerevisiae* with α-ketoglutarate binding before AcCoA and CoA released before homocitrate. Oxaloacetate is also a substrate for HCS, but with lower affinity than α-ketoglutarate. In agreement with the ordered kinetic mechanism desulfo-CoA is uncompetitive and citrate is competitive vs α-ketoglutarate. Varying AcCoA, citrate is a noncompetitive inhibitor as predicted, but CoA is noncompetitive vs AcCoA suggesting binding of CoA to E:homocitrate and E:α-ketoglutarate. The product CoA behaves in a manner identical to the dead-end analogue desulfo-CoA, suggesting an E:α-ketoglutarate:CoA dead-end complex. Data further suggest an irreversible reaction overall, in agreement with the downhill nature of the reaction as a result of homocitryl-CoA hydrolysis. Fluorescence titration data generally agree with the steady state data, but show finite binding of CoA and AcCoA to free enzyme, suggesting that the mechanism may be random with a high degree of synergism of binding between the reactants.

Homocitrate synthase (HCS[1]) [3-hydroxy-3-carboxyadipate 2-oxoglutarate-lyase (CoA-acetylating), EC 4.1.3.21] is the first and regulated enzyme of the α-aminoadipate pathway for the biosynthesis of lysine. The pathway is unique to higher fungi such as the human pathogens *Candida albicans*, *Cryptococcus neoformis*, and *Aspergillus fumigatus* and the plant pathogen *Magnaporthe grisea*. The uniqueness of the α-aminoadipate pathway makes it a potential target for the design of the highly specific antimycotic agents (*1*−*5*).

The pathway begins with the condensation of α-ketoglutarate with AcCoA to yield homocitrate and coenzyme A with the intermediacy of a homocitryl-CoA intermediate (*2*−*5*). There are two isozymes of HCS from *Saccharomyces cerevisiae* (cytosolic and mitochondrial), and both are feedback inhibited by lysine, the pathway end product, and the expression of the cytosolic isozyme is repressed by lysine (*6*). HCS activity may also be regulated by divalent metal ions in the presence of CoA (*7*).

There are few studies on the kinetic mechanism of the HCS. An ordered kinetic mechanism has been proposed for the HCS from *Saccharomycopsis lipolytica* with α-ketoglutarate binding before AcCoA (*8*). The authors reported a sigmoid saturation curve for AcCoA. A sigmoid saturation curve for AcCoA was also reported for the enzyme from *Penicillium chrysogenum* (*9*). It has been also demonstrated that the HCS from *Thermus thermophilus* is capable of catalyzing the reaction using oxaloacetate in place of α-ketoglutarate as a substrate, and thus behaves as a citrate synthase (*10*).

The HCS from *S. cerevesiae* is unstable as isolated (*11*). Stabilization of the HCS from *S. cerevisiae* provided us with an enzyme with a longer half-life (*11*) making it possible to carry out detailed kinetic studies. In this paper, we report the kinetic mechanism of the HCS from *S. cerevisiae*.

MATERIALS AND METHODS

Materials. All chemicals were of the highest grade commercially available. α-Ketoglutarate, oxaloacetate, citrate, dichlorophenol indophenol (DCPIP), AcCoA, CoA, desulfo-CoA, α-cyclodextrin, L-glutamate, succinic acid, and γ-ketopimelate were obtained from Sigma. KCl, GdmCl, and glycerol were purchased from Fisher Scientific. $(NH_4)_2SO_4$ was obtained from Fluka, and Hepes was from Amresco. Imidazole was obtained from Research Organics.

The concentrations of AcCoA, CoA, and desulfo-CoA were adjusted spectrophotometrically (ϵ_{260}, 16.4 mM^{-1} cm^{-1}). A solution of AcCoA in ddH_2O is stable, without any significant hydrolysis, for at least a month if kept at −21 °C. The concentration of DCPIP preparations was also adjusted spectrophotometrically (ϵ_{600}, 19.1 mM^{-1} cm^{-1}).

Assays of Homocitrate Synthase Activity. Cell growth, HCS expression, and purification were performed as previously described (*11*). A typical assay for the HCS using the DCPIP method (monitoring the decrease in absorbance at 600 nm upon DCPIP reduction) is as described with slight modifications (*11*). The final volume of the assay was 0.5 mL and contained 50 mM Hepes, pH 7.5 (adjusted by KOH), and variable concentrations of α-Kg and AcCoA (~K_m or

† This work was supported by a grant in aid from the Office of the Research and Administration at the University of Oklahoma and by the Grayce B. Kerr endowment to the University of Oklahoma for the research of P.F.C.

* Corresponding author. E-mail: pcook@chemdept.chem.ou.edu. Tel: 405-325-4581. Fax: 405-325-7182.

[1] Abbreviations: HCS, homocitrate synthase; Hepes, 4-(2-hydroxyethyl)-1-piperazine-ethanesulfonic acid; CoA, coenzyme A.; Gdm, guanidinium; TCA, tricarboxylic acid; AcCoA, acetyl-CoA.; α-Kg, α-ketoglutarate; Hc, homocitrate; OAA, oxaloacetic acid; C, competitive; NC, noncompetitive; UC, uncompetitive.

10.1021/bi048766p CCC: $27.50
Published on Web 08/25/2004

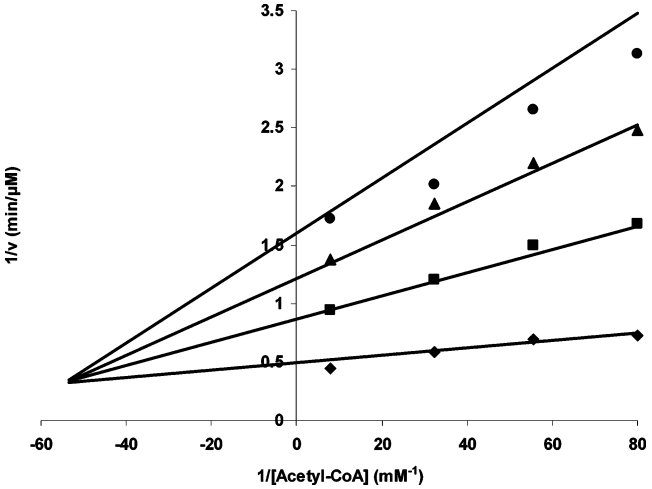

FIGURE 1: Initial velocity double-reciprocal plot for the HCS reaction. The concentrations of AcCoA are as plotted, while α-Kg is fixed at 10 mM (◆), 2.5 mM (■), 1.46 mM (▲), and 1 mM (●). The solid lines are theoretical data based on the fit to eq 1, while the points are experimental. Note that the experimental values measured using 1 mM α-Kg are higher than the predicted values due to the activating effect of monovalent cations on the HCS (unpublished data).

$\sim 20K_m$) and 0.1 mM DCPIP. All assays were carried out at 25 °C. Reactions were thermally equilibrated to allow for completion of the reaction between the small amount of CoA in the AcCoA solution and DCPIP before adding the enzyme to the reaction mixture. It should be noted that inhibition patterns for CoA could not be studied using the DCPIP assay. Therefore, the disappearance of absorbance at 232 nm (reflecting the thioester bond of AcCoA) was monitored in these cases (*11*). The decrease in absorbance at 232 nm ($\Delta\epsilon_{232} = 4.5$ mM^{-1} cm^{-1}) was monitored upon addition of the HCS using the 0.4 cm path length cuvette (NSG Precision Cells, Inc.).

In order to dissolve the precipitated α-cyclodextrin in the stabilized HCS suspension (*11*) glycerol was added to a final concentration of 10%. A dilute enzyme solution prepared using this method is stable at room temperature up to 3 h, after which the enzyme begins to lose activity.

Initial Velocity Studies. As described in the enzyme assay section, the DCPIP method was used to study initial velocity patterns with the exception of those in which CoA was present. The initial rate was measured as a function of AcCoA concentration (0.0125−0.125 mM) and a fixed concentration of α-Kg, and the experiment was then repeated at several additional α-Kg concentrations (1−10 mM). A similar experiment was carried out with OAA (10−50 mM) in place of α-Kg using the same variable concentrations of AcCoA at different fixed concentrations of OAA. Data in both cases were fitted to eq 1 for a sequential mechanism as represented using Cleland's nomenclature (*12*),

$$v = \frac{\mathrm{V}\mathbf{AB}}{K_{ia}K_b + K_a\mathbf{B} + K_b\mathbf{A} + \mathbf{AB}} \quad (1)$$

where v and V are initial and maximum rates, **A** and **B** are reactant concentrations, K_{ia} is the dissociation constant for A, and K_a and K_b are the Michaelis constants for **A** and **B**, respectively.

A point that must be considered when carrying out inhibition studies is related to the effect of monovalent ions on the HCS reaction. The behavior of HCS is complicated in the presence of monovalent and divalent cations (unpublished experiments). The major source of these ions is from the titrant used to adjust the pH of buffer and carboxylic acid substrate solutions. In addition, the presence of NH_4^+ in the stabilization buffer for HCS (*11*) is a source of monovalent ions. The activating effect of the NH_4^+ is obvious in Figure 1 at the lowest α-Kg concentration where the reciprocal values of the experimental data points are lower than the predicted values (solid line). This effect introduces some (manageable) error in data analysis. In general, when monovalent cations are not a subject of kinetic studies, their concentration should not exceed 50 mM.

Inhibition Studies. Inhibition patterns were obtained by measuring the initial rate at different concentrations of one reactant, a fixed concentration of the second reactant equal to K_m, and a fixed concentration of the inhibitor. The experiment was then repeated at several different fixed concentrations of the inhibitor (including zero). Dependent on whether the inhibition was competitive, noncompetitive, or uncompetitive, data were fitted to eqs 2−4.

$$v = \frac{V\mathbf{A}}{K_a\left(1 + \frac{\mathbf{I}}{K_{is}}\right) + \mathbf{A}} \quad (2)$$

$$v = \frac{V\mathbf{A}}{K_a\left(1 + \frac{\mathbf{I}}{K_{is}}\right) + \mathbf{A}\left(1 + \frac{\mathbf{I}}{K_{ii}}\right)} \quad (3)$$

$$v = \frac{V\mathbf{A}}{K_a + \mathbf{A}\left(1 + \frac{\mathbf{I}}{K_{ii}}\right)} \quad (4)$$

In eqs 2−4 K_{is} and K_{ii} are slope and intercept inhibition constants, respectively, **I** is the concentration of inhibitor, and all other terms are as defined above.

Fluorescence Determination of the HCS−Ligand Dissociation Constant. Fluorescence spectra were measured as previously described (*11*). Emission spectra were measured from 310 to 400 nm with the excitation monochromator fixed at 298 nm. Spectra were recorded on a Shimadzu RF-5301 PC spectrofluorometer equipped with circulating water bath to maintain the temperature at 25 °C. Fluorescence quartz cuvettes with a volume of 1 mL and a path length of 1 cm were used to measure sample and blank spectra. Excitation and emission slit widths were set to 1.5 and 5 nm, respectively. Because all of the reagents and buffer components have no absorbance above 310 nm, the inner filter effect is negligible under conditions used for taking the spectra.

The final buffer composition used to measure the spectra contained 55 mM Hepes (adjusted to pH 7.5 with KOH), 150 mM $(NH_4)_2SO_4$, 25 mM GdmCl, 25 mM α-cyclodextrin, 8 mM KCl, and 5 mM imidazole. All samples contained enzyme at a concentration of 55 μg/mL. Compounds used for fluorescence studies were α-Kg, OAA, AcCoA, and CoA that were added sequentially from low to high concentration to both the blank and sample from a stock solution of 1 M for α-Kg, 100 mM for OAA, 5 mM for AcCoA, and 8.6 mM for CoA. The final total dilution in each case was 1.07 (α-Kg), 1.08 (OAA), 1.10 (AcCoA), and 1.06 (CoA), and all the data were corrected for dilution.

Table 1: Kinetic Parameters for HCS

parameter	A = α-Kg	A = OAA
K_a (mM)	3.3 ± 0.2	25.5 ± 0.1
K_b (μM)	2.4 ± 0.2	1.30 ± 0.01
K_{ia} (mM)	25.1 ± 2.5	140 ± 1
V/E_t (s^{-1})	0.60 ± 0.03	0.30 ± 0.02
V/K_aE_t (M^{-1} s^{-1})	180 ± 14	9.8 ± 0.7
V/K_bE_t (M^{-1} s^{-1})	(2.5 ± 0.2) × 10^5	(2.0 ± 0.1) × 10^5

To calculate the K_d based on the fluorescence intensity, data were fitted to the equation for a rectangular hyperbola shown in eq 5,

$$\Delta F = \frac{\Delta F_{max}\mathbf{L}}{K_d + \mathbf{L}} \quad (5)$$

where ΔF is the change in intrinsic tryptophan fluorescence upon addition of ligand to enzyme, ΔF_{max} is the maximum change in fluorescence at infinite ligand concentration, L is ligand concentration and K_d is the dissociation constant for the enzyme−ligand complex.

Data Analysis. Initial rates and fluorescence intensity changes were plotted as reciprocal plots vs substrate or ligand concentration, and all plots and replots were linear. Data were fitted using the appropriate equations and the Marquardt−Levenberg algorithm supplied with the EnzFitter program from BIOSOFT, Cambridge, U.K. Rate, kinetic, and dissociation constants and their corresponding standard errors were estimated using a simple robust weighing method for the activity or affinity of the enzyme by fitting the curves to the data either in the absence or in the presence of inhibitors or ligands.

RESULTS

Initial Velocity Studies. The initial velocity pattern obtained by varying the concentration of α-Kg at different fixed concentrations of AcCoA is shown in Figure 1. The lines intersect to the left of the vertical axis consistent with the sequential Bi Bi mechanism (*13*). Data could not be obtained in the reverse reaction direction because of the irreversibility of the reaction (see below). However, the inhibition patterns provide a great deal of information about the sequential mechanism.

An intersecting pattern is also observed when OAA is used as an α-Kg substrate analogue (data not shown). Thus, HCS is capable of catalyzing a reaction that is specific to citrate synthase from the TCA cycle, although homocitrate synthase has no homology to citrate synthase in terms of sequence and probably three-dimensional structure (citrate synthase has an all-helical structure while the structure of homocitrate synthase is predicted to contain an α/β TIM barrel domain (*11*, *14*)). Kinetic parameters for HCS using either α-Kg or OAA are shown in Table 1.

The V/E_t values obtained with α-Kg and OAA are very similar, but V/KE_t values differ by more than an order of magnitude with $V/K_{\alpha-Kg}E_t > V/K_{OAA}E_t$. There is no difference in terms of specificity of the HCS for AcCoA using either α-Kg or OAA.

Product Inhibition Studies. The only product inhibition patterns obtained were with CoA, which is UC vs α-Kg and NC vs AcCoA, Table 2. The K_i of 20 μM for CoA suggests that it still binds with reasonably high affinity without the acetyl group.

Dead-End Inhibition Studies. On the basis of preliminary studies, HCS did not show any detectable inhibition by 10 mM L-glutamate, 50 mM γ-ketopimelate, or 50 mM succinate (data not shown).

Dead-end inhibitors are invaluable in establishing order of binding in an enzyme mechanism (*13*). Desulfo-CoA was used as a dead-end analogue of AcCoA, and it is NC against AcCoA and UC against α-Kg. The uncompetitive inhibition against α-Kg suggests an ordered mechanism with α-Kg binding prior to AcCoA. The noncompetitive inhibition by CoA and desulfo-CoA suggests two combinations by the two inhibitors, one identical to the enzyme form to which AcCoA combines, and a second on the product side of the reaction, likely the E:Hc form of the enzyme. The lack of a slope effect in the case of the inhibition by CoA with α-Kg varied at a low AcCoA concentration suggests an irreversible reaction consistent with the downhill nature of the reaction as a result of the hydrolysis of the intermediate homocitryl-CoA.

Citrate was used as a dead-end analogue of α-Kg, and it is C vs α-Kg and NC vs AcCoA. Data are consistent with the proposed ordered addition of α-Kg before AcCoA with a dead-end E:α-Kg:CoA complex. All kinetic constants are summarized in Table 2.

Fluorescence Studies. In order to further test the proposed kinetic mechanism, fluorescence titrations were utilized to estimate the dissociation constants for enzyme−reactant complexes. Table 3 gives a list of the dissociation constants measured. All of the ligands quench the fluorescence

Table 2: Inhibition Kinetic Constants for Product and Dead-End Inhibitors of HCS

varied substrate	fixed substrate	inhibitor	K_{is}[a] (mM)	K_{ii}[a] (mM)	inhibition pattern
α-Kg	AcCoA (0.031 mM)	citrate	13.5 ± 1.0		C
AcCoA	α-Kg (5 mM)	citrate	19 ± 2 (17 ± 2)	200 ± 60 (74 ± 24)	NC
α-Kg	AcCoA (0.031 mM)	desulfo-CoA		0.021 ± 0.001	UC
AcCoA	α-Kg (5 mM)	desulfo-CoA	0.014 ± 0.002 (0.0023 ± 0.0004)	0.18 ± 0.05 (0.11 ± 0.03)	NC
α-Kg	AcCoA (0.031 mM)	CoA		0.0240 ± 0.0005	UC
AcCoA	α-Kg (5 mM)	CoA	0.008 ± 0.002 (0.0013 ± 0.0003)	0.033 ± 0.009 (0.020 ± 0.006)	NC

[a] The values in parentheses are the corrected values for the fixed reactant where applicable.

Table 3: Dissociation Constants of Ligand−HCS Complexes from Fluorescence Titration

ligand	K_d (mM)
α-Kg	26 ± 1
α-Kg (+0.5 mM CoA)	111 ± 1
OAA	3.70 ± 0.02
CoA	0.17 ± 0.01
AcCoA	0.45 ± 0.01

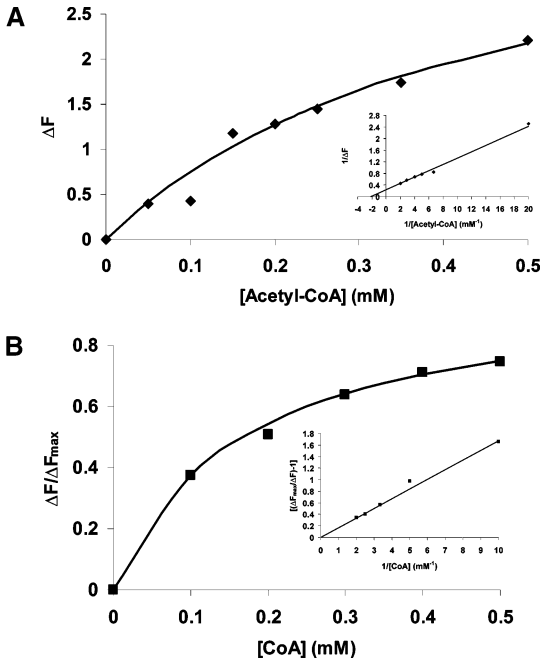

FIGURE 2: (A) Determination of the K_d for AcCoA via fluorescence titration. A plot of ΔF vs the concentration of AcCoA is shown. The inset shows a double reciprocal plot of the data, with the x-intercept equal to $-1/K_d$. (B) Determination of the K_d for CoA via fluorescence titration. The curves are theoretical based on a fit to eq 5, while points are experimental in both cases.

emission of the single tryptophan of HCS with the exception of CoA, which gives a slight enhancement of fluorescence (*11*).

Although AcCoA binds to free HCS, its K_d (450 μM) (Figure 2) is much higher than its K_m (2 μM). The K_d for E:α-Kg, however, is identical within error to the K_{ia} value reported in Table 1. Although CoA binds better to E than does AcCoA (3-fold), it still has a weaker affinity than it does to the E:Hc complex (8−9-fold). Interestingly, the presence of CoA (3 times its K_d) decreases the affinity of α-Kg by 4-fold, while OAA binds better to free HCS than does α-Kg (7-fold).

DISCUSSION

The initial velocity pattern gives a family of lines that intersect to the left of the ordinate suggesting a sequential kinetic mechanism for HCS. The ordered nature of the mechanism is suggested by the UC inhibition by desulfo-CoA and CoA vs α-Kg. In both cases these inhibitors are NC vs AcCoA, the substrate they mimic structurally. Data thus indicate that the inhibitors combine with two separate enzyme forms, one the same as that to which AcCoA binds, the E:α-Kg complex, and a second, likely the normal product complex to which CoA binds, E:homocitrate. In a reversible reaction, binding of CoA to the E:Hc complex would give

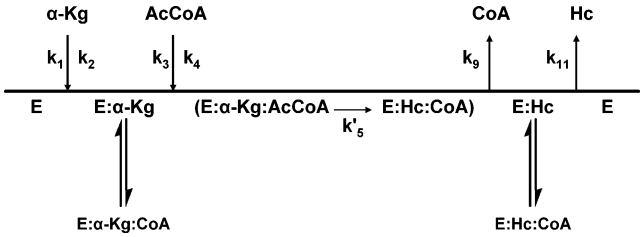

FIGURE 3: Proposed kinetic mechanism for the HCS. E represents the HCS. Kinetic data suggest that the reaction is irreversible in agreement with the thermodynamics of the reaction. CoA (and desulfo-CoA) can bind to both E:α-Kg and E:Hc forms of the enzyme, while citrate binds to E. k'_5 is the net catalysis rate and is defined as $k_5k_7/(k_6 + k_7)$.

NC inhibition vs both substrates in an ordered mechanism as a result of reversal of the reaction. In this case, however, equilibrium is far to the right as a result of hydrolysis of the intermediate homocitryl CoA, and the reaction is practically irreversible. (Homocitrate and CoA are products since the absorbance of the thioester bond decreases as AcCoA is used up and the appearance of CoA can be monitored using the DCPIP assay (*11*).) Both CoA and desulfo-CoA can thus be treated as dead-end inhibitors. An analogue of the first substrate bound in an ordered mechanism would be expected to be C vs α-Kg and NC vs AcCoA, as is observed for citrate. A kinetic mechanism can thus be proposed as shown in Figure 3. The mechanism is ordered with α-Kg binding before AcCoA and with CoA released before Hc. The reaction is practically irreversible, and the product CoA can bind to the E:α-Kg and E:Hc complexes.

Quantitative Analysis of Inhibition Data. Since all inhibitors, including CoA, can be treated as dead-end inhibitors, correction of the observed K_i values for the fixed variable substrate should give the same true K_i values whichever of the substrates is varied. The competitive inhibition by citrate vs α-ketoglurate gives the true K_i for the inhibitor for the E:citrate complex, 14 μM. With AcCoA varied, however, the observed K_{is} and K_{ii} values must be corrected for the concentration of the fixed substrate. Given the rate equation for the ordered kinetic mechanism, eq 1, the presence of the inhibitor adds a $(1 + \mathbf{I}/K_i)$ term to each of the denominator terms representing free enzyme, $K_{ia}K_b$ and $K_a\mathbf{B}$, to give eq 6, where K_i is the intrinsic dissociation constant for EI.

$$v = \frac{V\mathbf{AB}}{(K_{ia}K_b + K_a\mathbf{B})\left(1 + \frac{\mathbf{I}}{K_i}\right) + K_b\mathbf{A} + \mathbf{AB}} \quad (6)$$

With **B** varied, eq 6 in double reciprocal form is given by eq 7.

$$\frac{1}{v} = \left[\left(\frac{K_{ia}K_b}{V\mathbf{A}}\right)\left(1 + \frac{\mathbf{I}}{K_i}\right) + \frac{K_b}{V}\right]\left(\frac{1}{\mathbf{B}}\right) + \left(\frac{K_a}{V\mathbf{A}}\right)\left(1 + \frac{\mathbf{I}}{K_i}\right) + \frac{1}{V} \quad (7)$$

The observed or appK_i is then obtained from the expressions for slope and intercept vs **I** when the slope is zero. As an example, the expression for the slope inhibition constant is derived below.

$$\text{slope} = \left(\frac{K_{ia}K_b}{V\mathbf{A}} + \frac{K_b}{V}\right) + \left(\frac{K_{ia}K_b}{VK_i\mathbf{A}}\right)\mathbf{I} \quad (8)$$

and with slope equal to zero

$$\mathbf{I} = \text{app}K_i = K_i\left(1 + \frac{\mathbf{A}}{K_{ia}}\right) \quad (9)$$

where appK_i is the measured K_{is} value given in Table 2. The expression for K_{ii} can be derived in a similar manner, and the true K_i can be calculated. The calculated K_i values of 13 μM and 17 μM agree very well, Table 2 (values in parentheses). Although the corrected K_{is} and K_{ii} values for the inhibition by citrate vs **B** (Table 2) are different, they are the same order of magnitude, and the value obtained from K_{ii} has a high error associated with it.

Inhibition by desulfo-CoA or CoA results from binding to E:α-Kg, represented by the $K_b\mathbf{A}$ term, and a form of the enzyme present at saturating concentrations of both reactants, represented by the **AB** term. Equation 1 can thus be modified as follows to give the rate equation for inhibition by either desulfo-CoA or CoA.

$$v = \frac{V\mathbf{AB}}{K_{ia}K_b + K_a\mathbf{B} + K_b\mathbf{A}\left(1 + \frac{\mathbf{I}}{K_{i1}}\right) + \mathbf{AB}\left(1 + \frac{\mathbf{I}}{K_{i2}}\right)} \quad (10)$$

In eq 7, K_{i1} is the intrinsic K_i for E:α-Kg:I, but K_{i2} is an apparent K_i with a value determined by the amount of the E:Hc complex that builds up in the steady state at saturating substrate concentrations. Values for K_{i1} and K_{i2} can be evaluated as above, from the noncompetitive inhibition vs AcCoA, giving 1 μM and 20 μM, respectively, for CoA, and 2 μM and 110 μM, respectively, for desulfo-CoA. Thus, CoA binds better by a factor of 2 to E:α-Kg.

The observed K_{ii} from the UC inhibition pattern obtained for CoA or desulfo-CoA vs α-Kg cannot so easily be evaluated. The expression for K_{ii} is given in eq 11.

$$K_{ii} = \frac{\left(1 + \frac{K_b}{\mathbf{B}}\right)}{\left(\frac{1}{K_{i2}} + \frac{K_b}{\mathbf{B}K_{i1}}\right)} \quad (11)$$

Substituting values for **B**, K_b, and the calculated values for K_{i1} and K_{i2} from Table 2 in eq 11 gives K_{ii} values of 25 μM and 19 μM for desulfo-CoA and CoA, respectively, in excellent agreement with the measured values of 21 μM and 24 μM, respectively. Data are consistent with the proposed ordered kinetic mechanism.

If the assumption is made that $K_{i1} = K_{i2}$, perhaps reasonable due to the similarity in the structures of the desulfo-CoA to CoA and AcCoA, the amount of E:Hc that builds up in the steady state can be estimated. The ratio K_{i1}/K_{i2} is directly proportional to the amount of E:Hc that builds up in the steady state. Estimates that are obtained from CoA and desulfo-CoA are 2−5%, suggesting a significant but small contribution of the release of homocitrate to overall rate limitation under V_{max} conditions. A reasonable kinetic mechanism for HCS under V_{max} conditions is given below,

$$\text{E:α-Kg:AcCoA} \underset{k_6}{\overset{k_5}{\rightleftharpoons}} \text{E:HcCOA} \xrightarrow{k_7} \text{E:Hc:CoA} \xrightarrow{k_9} \text{E:Hc} \xrightarrow{k_{11}} \quad (12)$$

where HcCoA is homocitryl-CoA, k_5 and k_6 represent formation of HcCoA and its decomposition to reactants α-Kg and AcCoA, k_7 represents hydrolysis of HcCoA to products Hc and CoA, and k_9 and k_{11} represent release of CoA and Hc, respectively. The expression for V_{max} is then given below in terms of enzyme forms that build up in the steady state.

$$V = \frac{E_t}{\frac{k_6 + k_7}{k_5k_7} + \frac{1}{k_7} + \frac{1}{k_9} + \frac{1}{k_{11}}} = \frac{E_t}{\text{E:α-Kg:AcCoA} + \text{E:HcCoA} + \text{E:Hc:CoA} + \text{E:Hc}} \quad (13)$$

If E:Hc is 2−5% of the total enzyme at saturating substrates, the remaining 95−98% is made up of some combination of the remaining enzyme forms. The determination of distribution will have to await further studies including those using isotope effects to probe the chemical steps.

Fluorescence Binding Studies. The dissociation constant for the E:α-Kg complex obtained from steady state kinetic studies (K_{ia} in Table 2) is identical to that obtained from fluorescence titration, Table 3. However, fluorescence data, Table 3, indicate finite binding of AcCoA and CoA to free enzyme. The K_d for E:AcCoA (450 μM), Table 3, is more than 200 times higher than the K_m for AcCoA (2 μM), Table 2. In addition, the K_d for E:CoA (170 μM), Table 3, is almost 100 times higher than its K_i for the E:α-Kg:CoA complex (1 μM), Table 2. It is thus possible that the kinetic mechanism of HCS is random with a high degree of synergism of binding between α-Kg and AcCoA. (There is a similar but less pronounced difference in the dissociation constant for enzyme−α-Kg complex and its K_m.) Since the ordered mechanism suggested for HCS may arise as a result of a high degree of synergism (*13*) as described above, we suggest a preferred ordered mechanism. Although one would expect NC inhibition by CoA vs α-Kg in this case, the concentration of CoA used in these studies would not be sufficient to generate a significant slope effect as a result of CoA binding to E at low α-Kg.

Interestingly, the binding of CoA (in contrast to AcCoA) to the HCS enhances the intrinsic fluorescence of the HCS, suggesting a conformational change that alters the microenvironment of the strategically located single tryptophan residue of the enzyme toward an increased hydrophobicity. The reasoning for this phenomenon may be the closure of the active site upon binding of the CoA to the free enzyme or E:α-Kg complex, consistent with the increased K_d of E:α-Kg:CoA, Table 3.

Active Site Specificity and Kinetic Mechanism. On the basis of the inhibition studies and data obtained with the alternative substrate OAA, some information can be provided on the active site of HCS. As shown in Table 3, the dissociation constant (K_d) of E:OAA (3.7 mM) is less than that for E:α-Kg (25 mM), suggesting that the binding of OAA is favored by about 1.1 kcal/mol. On the other hand the second-order rate constant (V/KE_t) is a factor of 16 higher for α-Kg than for OAA. This reflects a kinetic preference for binding of α-Kg of about 1.7 kcal/mol. (The V/K for the first substrate in an ordered mechanism is its rate constant for combination with enzyme. For a simple, single step

binding process this rate constant would be expected to equal the diffusion limit of 10^8 M^{-1} s^{-1}. The low values observed for both substrates suggest a multistep binding process with the first reactant inducing a conformational change in enzyme to facilitate binding of the second substrate.)

The value of K_a/K_{ia} is almost the same for both α-Kg and OAA, and the crossover point for the intersecting initial velocity pattern is above the horizontal axis for both substrates due to be less than unity of the K_a/K_{ia} ratio. The kinetically determined K_{ia} for E:α-Kg is the same as the fluorescently determined K_d. However, this is not the case for OAA. This discrepancy may be explained by some randomness in the kinetic mechanism in which OAA can bind productively to the E:AcCoA complex (preliminary data agree with this suggestion). It is also possible that, with OAA as a substrate, some nonproductive binding is observed. However, in this case a decrease in K_m and V_{max} would be expected for OAA compared to α-Kg, and this is not observed.

The low K_d for OAA binding relative to α-Kg, see above, and inability of the enzyme to accommodate the carboxyethyl moiety of the γ-ketopimelate suggest that α-Kg, when bound, may be somewhat strained, i.e., it does not bind in an extended conformation, and the shorter OAA may fit better in the active site. The fact that succinate is not an effective inhibitor suggests that the α-carbonyl group is important for binding, as expected since the carbonyl oxygen must be protonated as homocitryl CoA is formed. In the case of HCS from *T. thermophilus*, α-ketoadipate and α-ketoisovalerate have no effect on enzyme activity as reported (*10*), so that chains longer than 5 carbons or with bulkier side chains are not accommodated. Additional kinetic experiments are required to better understand active site specificity.

ACKNOWLEDGMENT

We thank Dr. W. E. Karsten for his insightful discussion of the results. We also thank Dr. Elena Zgurskaya for the use of the spectrofluorometer.

REFERENCES

1. Johansson, E., Steffens, J. J., Lindqvist, Y., and Schneider, G. (2000) Crystal structure of Saccharopine reductase from *Magnaporthe grisea*, an enzyme of the α-aminoadipate pathway of lysine biosynthesis, *Structure 8*, 1037−1047.
2. Bhattacharjee, J. K. (1992) Evolution of α-aminoadipate pathway for the synthesis of lysine in fungi, in *Evolution of Metabolic Function* (Mortlock, R. P., Ed.) pp 47−80, CRC Press, Boca Raton.
3. Bhattacharjee, J. K. (1985) α-Aminoadipate pathway for the biosynthesis of lysine in lower eukaryotes, *Crit. Rev. Microbiol. 12*, 131−151.
4. Umbarger, H. E. (1987) Amino acid biosynthesis and its regulation, *Annu. Rev. Biochem. 47*, 532−606.
5. Vogel, H. J. (1960) Two modes of lysine synthesis among lower fungi: evolutionary significance, *Biochim. Biophys. Acta 41*, 172−173.
6. Ramos, F., Verhasselt, P., Feller, A., Peeters, P., Wach, A., Dubois, E., and Volckaert, G. (1996) Identification of a gene encoding a homocitrate synthase isoenzyme of *Saccharomyces cerevisiae*, *Yeast 12*, 1315−1320.
7. Tracy, J., and Kohlhaw, G. (1975) Reversible, coenzyme-A-mediated inactivation of biosynthesis condensing enzymes in yeast: A possible regulatory mechanism, *Proc. Natl. Acad. Sci. U.S.A. 72*, 1802−1805.
8. Gaillardin, G. M., Poirier, L. and Heslot, H. (1976) A kinetic study of homocitrate synthase activity in the yeast *Saccharomycopsis lipolytica*, *Biochim. Biophys. Acta 422*, 390−406.
9. Jaklitsch W. M., and Kubicek, C. P. (1990) Homocitrate synthase from *Penicillium chrysogenum*, localization, purification of the cytosolic isoenzyme, and sensitivity to lysine, *Biochem. J. 269*, 247−253.
10. Wulandari, A. P., Miyazaki, J., Kobashi, N., Nishiyama, M., Hoshino T., and Yamane, H. (2002) Characterization of bacterial homocitrate synthase involved in lysine biosynthesis, *FEBS Lett. 522*, 35−40.
11. Andi, B., West, A. H., and Cook, P. F. (2004) Stabilization and characterization of histidine-tagged homocitrate synthase from *Saccharomyces cerevisiae*, *Arch. Biochem. Biophys. 421*, 243−254.
12. Cleland, W. W. (1963) The kinetics of enzyme-catalyzed reactions with two or more substrates or products I. Nomenclature and rate equations, *Biochim. Biophys. Acta 67*, 104−137.
13. Cleland, W. W. (1977) Determining the chemical mechanisms of enzyme-catalyzed reactions by kinetic studies, *Adv. Enzymol. 45*, 273−387.
14. Berman, H. M., Westbrook, J., Feng, Z., Gilliland, G., Bhat, T. N., Weissig, H., Shindyalov, I. N., and Bourne, P. E. (2000) The protein data bank, *Nucleic Acids Res. 28*, 235−242.

BI048766P